J. Fluid Mech. (1980), *vol.* 97, *part* 4, *pp.* 743–758
Printed in Great Britain

Heat source-driven thermal convection at arbitrary Prandtl number

By F. B. CHEUNG

Reactor Analysis and Safety Division, Argonne National Laboratory,
9700 South Cass Avenue, Argonne, Illinois 60439

(Received 18 January 1979 and in revised form 30 July 1979)

A theoretical investigation is made of turbulent thermal convection in a horizontally infinite layer of fluid confined between a rigid isothermal upper plate and a rigid adiabatic lower plate, driven by a temperature difference between the plates that is totally induced by volumetric heating of the layer. The dependence of upper surface Nusselt number, Nu, on both Prandtl number, Pr, and internal Rayleigh number, Ra_I, is obtained from considerations of the Boussinesq equations of motion. Also obtained is the dependence of various turbulence quantities upon distance from the upper plate. At a sufficiently high Rayleigh number, the present theory gives $Nu \sim Ra_I^{\frac{1}{5}}$ for large Pr and $Nu \sim Pr^{\frac{1}{2}} Ra_I^{\frac{1}{4}}$ for small Pr. At lower Rayleigh numbers, however, the Nusselt number is found to vary according to $Nu \sim (a - bRa_I^{-\frac{1}{11}})^{-1} Ra_I^{\frac{1}{5}}$, where a and b are coefficients dependent upon Pr. The asymptotic $Ra_I^{\frac{1}{5}}$ law tends to support the boundary layer instability model of Howard (1966), although significant deviation from the model is predicted by the present theory over the range of Rayleigh numbers explored experimentally (Kulacki & Nagle 1975; Kulacki & Emara 1977). Based upon the results of this study the empirical power-law representation of Nu is critically examined and found to be adequate within finite ranges of Ra_I. Comparison of the present flow situation is made with the corresponding case of turbulent Bénard convection.

1. Introduction

The process of turbulent thermal convection in a volumetrically heated horizontal fluid layer bounded below by a rigid zero-heat-flux surface and above by a rigid isothermal surface has recently received special attention both experimentally and theoretically, mainly because of its relevance to the post-accident heat-removal situation encountered in a hypothetical core-meltdown event in a nuclear power reactor. Such process differs from that of turbulent Bénard convection in that the total heat flux is not constant but varies across the layer. With the lower surface of the layer being thermally insulated, the flow has to bring all parts of the heat-generating fluid close to the upper surface to permit them to lose heat by conduction. As a result, the mechanism of turbulent heat transport in a horizontal layer heated from within is not quite the same as that heated from below. While the heat transfer properties of turbulent Bénard convection have been studied extensively (Malkus 1954; Priestley 1959; Kraichnan 1962; Herring 1964; Howard 1966; Spiegel 1971; Chu & Goldstein 1973; Garon & Goldstein 1973; Threlfall 1975; Long 1976*a*, *b*), the characteristic

0022–1120/80/4427-0000 $01.00

features of heat source-driven convection are less understood. A desire to seek a clear physical picture of the process provides the major motivation for this study.

Experimental work on turbulent thermal convection in heat-generating layers with thermal and hydrodynamic boundary conditions of interest to the present study is limited to the investigations of Fiedler & Wille (1971), Kulacki & Nagle (1975) and Kulacki & Emara (1977). All of these studies employed electrolytically heated water layers to measure the average Nusselt number, Nu, at the upper surface as a function of the internal Rayleigh number, Ra_I, defined in terms of the layer depth and the strength of volumetric heat generation. The results were presented in the form

$$Nu = \text{constant} \times Ra_I^m.$$

Fiedler & Wille reported a value of $m = 0{\cdot}228$ in the range $2 \times 10^5 \leqslant Ra_I \leqslant 6 \times 10^8$. A somewhat different value of $m = 0{\cdot}239$ was reported by Kulacki & Nagle for $1{\cdot}5 \times 10^5 \leqslant Ra_I \leqslant 2{\cdot}5 \times 10^9$ and $6{\cdot}21 \leqslant Pr \leqslant 6{\cdot}64$. Kulacki & Emara performed measurements in the range $1{\cdot}89 \times 10^3 \leqslant Ra_I \leqslant 2{\cdot}17 \times 10^{12}$ for $2{\cdot}75 \leqslant Pr \leqslant 6{\cdot}86$ and reported a value of $m = 0{\cdot}227$ similar to that obtained by Fiedler & Wille, but with a much lower value for the constant. Although the work of Kulacki & Emara covers a wide range of Rayleigh numbers, their data do not permit determination of the behaviour of the upper surface Nusselt number as the internal Rayleigh number approaches infinity. Whether the above observations are consistent with the asymptotic law of dependence of heat transport on Rayleigh number has yet to be examined. So far, there is no physical explanation on the $Nu - Ra_I$ relation over the range of Rayleigh numbers observed in laboratory experiments.

Very few theoretical studies have been made of the turbulent convection problem in question. In part, this is because of the fact that there are more unknowns than equations in the mathematical representation of the flow. The lack of experimental data on the detailed structure of turbulence imposes further difficulties on the task of solution. Fiedler & Wille performed an approximate analysis of the heat-transport problem in 1971. They appealed directly to the Prandtl mixing-length hypothesis to close the turbulent energy equation. Their analysis resulted in the prediction of the average Nusselt number at the upper surface but had to rely on estimates of the empirical constants resulting from their approach. Cheung (1977) employed a rather different phenomenological model to analyse the same problem. He considered the process of turbulent thermal convection to be well described by a local Rayleigh number of the flow, which was characterized by a local buoyancy difference and a local length scale. The former was related to a local temperature drop according to the Boussinesq approximation and the latter, to local distances from the upper and the lower walls. No account was made for the effect of Prandtl number. The approach was later shown to be applicable to transient convection situations (Cheung 1978*a*). None of these studies, however, provides a direct comparison between the processes of heat source-driven and Rayleigh–Bénard convection. Most recently, Cheung (1978*b*) and Bergholz, Chen & Cheung (1979) made use of the boundary-layer dominant aspect of turbulent flows to examine the reported heat-transfer data for internally, heated and bottom-heated layers. The common character of upper surface heat transfer in the two layers was demonstrated empirically by a simple boundary-layer type of analysis. Unfortunately, comparison between the fundamental physical features for the two processes cannot be made from considerations of the heat-transfer data alone.

In the present approach, the process of heat source-driven convection in the turbulent flow régime is investigated theoretically based upon systematic mathematical approximations to the Boussinesq equations of motion. The internal Rayleigh number of the layer is considered to be sufficiently high so that most of the change in mean temperature occurs in thin boundary-layer regions near the wall. Two asymptotic cases, one for high Prandtl number and the other for low, are treated in a manner similar to that of Kraichnan (1962). For high Prandtl number, we consider a thin conduction layer imbedded in a thick viscous layer; for low Prandtl number, the conduction layer is considered thicker. In either case, the behaviour of the velocity and temperature fields in the molecular boundary layers is studied separately from that in the turbulent core. Functional dependence of the upper surface heat transfer upon internal Rayleigh number and Prandtl number is then derived by matching of the flows in the two regions. Generalization of the functional expression is performed subsequently to the case of moderate Prandtl number. The local and overall heat transfer properties so obtained are compared with those of turbulent Bénard convection to identify the basic differences as well as similarities between the two motions. In addition, the behaviour of the upper surface Nusselt number as the internal Rayleigh number approaches infinity is determined. How and why the Nusselt number deviates from its asymptotic behaviour at lower Rayleigh numbers are discussed together with experiment.

2. Theoretical considerations

Consider the process of turbulent heat transport in a horizontally infinite layer of volumetrically heated fluid bounded below by a rigid, adiabatic surface and above by a rigid, isothermal surface. The strength of the volumetric heat generation is assumed to be spatially uniform and time invariant so that a statistically steady one-dimensional transport is maintained in the layer. The properties of the fluid are assumed to be constant except density variation in the buoyancy force. In natural units, the Boussinesq equations of motion are

$$(\partial/\partial t - \alpha\nabla^2)\,T = -(\mathbf{u}\,.\,\nabla)\,T + S/\rho_0 C_p, \tag{1}$$

$$(\partial/\partial t - \nu\nabla^2)\,\mathbf{u} = -(\mathbf{u}\,.\,\nabla)\,\mathbf{u} - \rho_0^{-1}\nabla P + \mathbf{k}g\beta T, \tag{2}$$

$$\nabla\,.\,\mathbf{u} = 0, \tag{3}$$

where $\mathbf{u}$ is the velocity vector, T the temperature, P the pressure, ρ_0 the mean density, S the volumetric rate of heat generation, C_p the specific heat, α the thermal diffusivity, ν the kinematic viscosity, g the gravitational acceleration, β the isobaric coefficient of thermal expansion, and $\mathbf{k}$ the unit vector in the vertical. In the above formulation, the zero of temperature is taken to be the mean temperature in the turbulent core. This is virtually the same as the lower surface temperature since the bottom is thermally insulated and no thermal boundary layer is present there. Note that the main driving force of the motion is represented by the term $S/\rho_0 C_p$. The temperature difference ΔT between top and bottom surfaces is merely a consequence of volumetric heating of the layer. Dimensional considerations of (1)–(3) indicate that the upper surface Nusselt number

$$Nu = \Phi L^2/\alpha\Delta T, \tag{4}$$

is a function of the Prandtl number, $Pr = \nu/\alpha$, and the internal Rayleigh number of the layer

$$Ra_I = g\beta\Phi L^5/2\alpha^2\nu, \tag{5}$$

where $\Phi = S/\rho_0 C_p$. Unlike the case of Rayleigh–Bénard convection, the upper surface heat transfer, SL, is a known quantity in the present case, the unknown being the temperature difference ΔT.

Assuming the flow to be statistically stationary and one-dimensional, the dependent variables may be decomposed into the mean and fluctuating parts, i.e.,

$$T = \overline{T} + \theta, \quad \overline{T} = \overline{T}(z), \quad \overline{\theta} = \overline{\mathbf{u}} = 0, \tag{6}$$

where z is the vertical co-ordinate measured upward from the lower surface. The governing equations become

$$\alpha d^2\overline{T}/dz^2 = \overline{dw\theta}/dz - \Phi, \tag{7}$$

$$(\partial/\partial t - \alpha\nabla^2)\,\theta = -w\,d\overline{T}/dz - [(\mathbf{u}.\nabla)\,\theta - \overline{(\mathbf{u}.\nabla)\,\theta}], \tag{8}$$

$$(\partial/\partial t - \nu\nabla^2)\,\mathbf{u} = -(\mathbf{u}.\nabla)\,\mathbf{u} - \rho_0^{-1}\nabla p + \mathbf{k}g\beta\theta, \tag{9}$$

where $p = P - \overline{P} - \rho_0\overline{w^2}$ is the fluctuating pressure and w is the velocity component in the vertical direction. Equation (7) may be integrated once to yield

$$-\alpha\,d\overline{T}/dz + \overline{w\theta} = \Phi z, \tag{10}$$

where the boundary condition at the insulated lower surface has been used to eliminate the constant of integration. Clearly, the sum of the molecular and convective heat fluxes is not a constant as in the case of Rayleigh–Bénard convection but proportional to the distance from the lower surface. To see how this affects the motion of the layer, let us examine briefly the turbulent kinetic energy equation. Multiplying both sides of (9) by $\mathbf{u}$ and taking the ensemble average of the resultant equation, we obtain

$$-\frac{d}{dz}\overline{[w(q^2 + p/\rho_0)} - \nu\,d\overline{q^2}/dz] + g\beta\overline{w\theta} - \epsilon = 0, \tag{11}$$

where $q^2 = \frac{1}{2}\mathbf{u}.\mathbf{u}$ is the turbulent kinetic energy and $\epsilon = \nu\overline{(\partial u_i/\partial x_j)^2}$ is the energy dissipation. The term $g\beta\overline{w\theta}$ represents the production of $\overline{q^2}$ and is directly proportional to $(\Phi z + \alpha\,d\overline{T}/dz)$. At a sufficiently high Rayleigh number, the gradient of the fluid temperature $d\overline{T}/dz$ is important only in a thin molecular boundary layer at the upper wall. Over the body of the layer, the temperature is practically constant. Therefore, the rate of production of $\overline{q^2}$ is not at the same level even in the core region but varies almost linearly with z in the layer, having a zero value at the bottom and a maximum near the top. It is conceivable that the present flow structure can be quite different from that of a Bénard layer.

3. High-Prandtl-number approximation

For $Pr \gg 1$, we may consider three different flow regions: the imbedded thermal boundary-layer region $L > z > L - \delta_t$, the viscous boundary-layer region $L - \delta_t > z > L - \delta_v$, and the turbulent core region $L - \delta_v > z > 0$. In the imbedded thermal boundary-layer region, we may assume that molecular transport dominates over the corresponding eddy transport. From (10), we expect

$$|\alpha\,d\overline{T}/dz| \sim |\Phi z| \quad \text{or} \quad \alpha\Delta T_t/\delta_t \sim \Phi L, \tag{12}$$

where ΔT_t is the temperature difference across the thermal boundary layer. In writing (12), we have made use of the assumption of $\delta_t/L \ll 1$ to set $z \simeq L$. The validity of this assumption will be discussed shortly. In addition, we expect from (8)

$$|\alpha\nabla^2\theta| \sim |w\,d\bar{T}/dz| \quad \text{or} \quad \alpha\langle\theta\rangle_t/\delta_t^2 \sim \langle w\rangle_t\,\Delta T_t/\delta_t, \tag{13}$$

where $\langle\ \rangle$ denotes the r.m.s. value and the subscript t refers to the thermal boundary layer. Finally, we assume that the viscous term and the buoyancy term in (9) are of the same order, i.e.,

$$|\nu\nabla^2\mathbf{u}| \sim |g\beta\theta| \quad \text{or} \quad \nu\langle w\rangle_t/\delta_t^2 \sim g\beta\langle\theta\rangle_t. \tag{14}$$

The above equations lead to

$$\delta_t \sim (g\beta)^{-\frac{1}{4}}\nu^{\frac{3}{4}}(\Phi L)^{-\frac{1}{4}}Pr^{-\frac{1}{2}}, \tag{15}$$

$$\Delta T_t \sim (g\beta)^{-\frac{1}{4}}\nu^{-\frac{1}{4}}(\Phi L)^{\frac{3}{4}}Pr^{\frac{1}{2}}. \tag{16}$$

From (5) and (15), we have

$$\delta_t/L \sim Ra_7^{-\frac{1}{4}}. \tag{17}$$

Hence $\delta_t/L \ll 1$ is a valid assumption at high Rayleigh numbers. Note that the lower surface temperature is taken to be zero in our convention, and that the upper surface temperature is equal to $-\Delta T$. From (16), the mean temperature at the edge of the thermal boundary layer may be expressed by

$$\bar{T}_{\delta_t} = C_1(g\beta)^{-\frac{1}{4}}\nu^{-\frac{1}{4}}(\Phi L)^{\frac{3}{4}}Pr^{\frac{1}{2}} - \Delta T, \tag{18}$$

where C_1 is a factor of proportionality and where we allow variation with Pr in a manner such that C_1 is independent of Pr as $Pr \to \infty$.

In the viscous boundary-layer region, molecular viscosity and eddy conductivity are considered to be dominant. If we assume $\delta_t < \delta_v \ll L$ and a finite correlation between w and θ, (10) may be approximated by

$$\overline{w\theta} \sim \Phi z \quad \text{or} \quad \langle w\rangle_v\langle\theta\rangle_v \sim \Phi L, \tag{19}$$

where the subscript v refers to the viscous boundary layer. The conditions for $\delta_t < \delta_v \ll L$ will be discussed. Here we may also assume a balance between the viscous and buoyancy terms in the vertical equation of motion, i.e.,

$$|\nu\nabla^2\mathbf{u}| \sim |g\beta\theta| \quad \text{or} \quad \nu\langle w\rangle_v/\delta_v^2 \sim g\beta\langle\theta\rangle_v, \tag{20}$$

but in (8) we assume

$$|w\,d\bar{T}/dz| \sim |\mathbf{u}\,.\,\nabla\theta| \quad \text{or} \quad \Delta T_v \sim \langle\theta\rangle_v, \tag{21}$$

where ΔT_v is the increment in temperature from the edge of the thermal boundary layer to the edge of the viscous boundary layer. In addition, we may assume that the production and dissipation terms in (11) are of the same order. Using the argument that the internal dynamics of turbulence must transfer energy from large scales to small scales (see for example Tennekes & Lumley 1972), the rate of dissipation of turbulent energy may be estimated according to the energy of the large eddies (which is of order $\langle w\rangle_v^2$) and their time scale (which is of order $\delta_v/\langle w\rangle_v$). We get

$$|g\beta\overline{w\theta}| \sim |\epsilon| \quad \text{or} \quad g\beta\Phi L \sim \langle w\rangle_v^3/\delta_v, \tag{22}$$

where the relation $\overline{w\theta} \sim \Phi L$ has been used. Manipulation of (19)–(22) leads to

$$\delta_v \sim (g\beta)^{-\frac{1}{4}} \nu^{\frac{1}{2}} (\Phi L)^{-\frac{1}{4}} \tag{23}$$

$$\Delta T_v \sim (g\beta)^{-\frac{1}{4}} \nu^{-\frac{1}{4}} (\Phi L)^{\frac{3}{4}}. \tag{24}$$

From (5), (15), and (23), we have

$$\delta_t/\delta_v \sim Pr^{-\frac{1}{2}} \quad \text{and} \quad \delta_v/L \sim Pr^{\frac{1}{2}} Ra_I^{-\frac{1}{4}}. \tag{25}$$

Hence $\delta_t < \delta_v \ll L$ is a valid assumption if the conditions $Pr \gg 1$ and $Ra_I \gg Pr^2$ are satisfied. We may now construct the near-field temperature profile $\overline{T}_v$ in the region $L-\delta_t > z > L-\delta_v$. From (18) and (24), we obtain

$$\overline{T}_v = C_1 (g\beta)^{-\frac{1}{4}} \nu^{-\frac{1}{4}} (\Phi L)^{\frac{3}{4}} Pr^{\frac{1}{2}} + (g\beta)^{-\frac{1}{4}} \nu^{-\frac{1}{4}} (\Phi L)^{\frac{3}{4}} f(\eta, Pr) - \Delta T, \tag{26}$$

where $\eta = (L-z)/\delta_v$ and f is independent of Pr as $Pr \to \infty$. The behaviour of $f(\eta, Pr)$ will be determined later.

Let us now investigate the turbulent core region. Here we expect eddy transport dominates over the corresponding molecular transport. If again we assume a finite correlation between w and θ, (10) may be approximated by

$$\overline{w\theta} \sim \Phi z \quad \text{or} \quad \langle w \rangle_c \langle \theta \rangle_c \sim (\Phi L)(z/L), \tag{27}$$

where the subscript c refers to the turbulent core. Outside the wall region, we may assume a balance between advection and buoyancy in (9), i.e.,

$$|(\mathbf{u}.\nabla)\mathbf{u}| \sim |g\beta\theta| \quad \text{or} \quad \langle w \rangle_c^2/(L-z) \sim g\beta \langle \theta \rangle_c, \tag{28}$$

whereas in (8) we assume

$$|w\, d\overline{T}/dz| \sim |\mathbf{u}.\nabla\theta| \quad \text{or} \quad \overline{T}_c \sim \langle \theta \rangle_c + C_2, \tag{29}$$

where $\overline{T}_c$ is the turbulent core temperature and C_2 is an integration factor. In writing (28), we have chosen $(L-z)$ as the appropriate length scale of mixing relative to the upper surface. From (27), (28) and (29), we get

$$\langle w \rangle_c \sim (g\beta)^{\frac{1}{3}} (\Phi L)^{\frac{1}{3}} L^{\frac{1}{3}} (z/L)^{\frac{1}{3}} (1-z/L)^{\frac{1}{3}}, \tag{30}$$

$$\langle \theta \rangle_c \sim (g\beta)^{-\frac{1}{3}} (\Phi L)^{\frac{2}{3}} L^{-\frac{1}{3}} (z/L)^{\frac{2}{3}} (1-z/L)^{-\frac{1}{3}}, \tag{31}$$

$$\overline{T}_c \sim (g\beta)^{-\frac{1}{3}} (\Phi L)^{\frac{2}{3}} L^{-\frac{1}{3}} [(z/L)^{\frac{2}{3}} (1-z/L)^{-\frac{1}{3}} + C_2], \tag{32}$$

where C_2 is a new integration factor and where we allow variation with Pr in a manner such that C_2 is independent of Pr as $Pr \to \infty$. Two important differences in turbulent core structure may now be distinguished between heat source-driven and Rayleigh–Bénard convection. First, relative to the upper surface, the r.m.s. vertical velocity varies according to $(L-z)^{\frac{1}{3}}$ in Bénard flow (Kraichnan 1962) whereas it varies according to $[z(L-z)]^{\frac{1}{3}}$ in the present case. Second, the turbulent core temperature varies according to $(L-z)^{-\frac{1}{3}}$ in Bénard convection whereas here it varies according to $z^{\frac{2}{3}}(L-z)^{-\frac{1}{3}}$. The two differences, however, become less and less significant as we approach from the interior core region to a region just outside the molecular boundary layer at the upper wall, where z (but not $L-z$) may be regarded to have a constant value of $\sim L$. Insofar as the near-field behaviour is concerned, the two convective processes are indeed similar (Cheung 1978*b*; Bergholz *et al.* 1979). For a given Pr, we may choose η and ξ as the two independent variables for the problem in question,

where ξ is defined by $\xi = \delta_v/L$. In terms of η and ξ, the far-field temperature profile may be constructed directly from (32). This is

$$\bar{T}_c = C_3(g\beta)^{-\frac{1}{3}}(\Phi L)^{\frac{2}{3}} L^{-\frac{1}{3}}[C_2 + (\eta\xi)^{-\frac{1}{3}}(1-\eta\xi)^{\frac{2}{3}}], \tag{33}$$

where C_3 is a proportionality factor dependent upon Pr.

Let us now match the expressions for the near-field and the far-field temperatures. Here we assume that, at high Rayleigh number (for which $\xi \ll 1$), there is a region of overlap (i.e. $\bar{T}_v = \bar{T}_c$) near the edge of the molecular boundary layer where $z \sim L - \delta_v$ or $\eta \sim 1$. Without experimental evidence, the existence of such an overlap region may be conceivable based upon the argument that molecular viscosity and eddy viscosity are of the same order there. For $\xi \ll 1$ and $\eta \sim 1$, (23), (26), and (33) together with the definition of ξ lead to

$$C_1 Pr^{\frac{1}{2}} + f - \Psi = C_2\xi^{\frac{1}{3}} + C_3\eta^{-\frac{1}{3}}[1 + O(\xi)], \tag{34}$$

where C_2 and C_3 are new proportionality factors dependent upon Pr and

$$\Psi = (g\beta)^{\frac{1}{2}}\nu^{\frac{1}{2}}(\Phi L)^{-\frac{3}{2}}\Delta T = \Psi(\xi, Pr). \tag{35}$$

Neglecting the higher-order term in (34) and rearranging, we obtain

$$f - C_3\eta^{-\frac{1}{3}} = \Psi - C_1 Pr^{\frac{1}{2}} + C_2\xi^{\frac{1}{3}} = C_4, \tag{36}$$

where C_4 is a parameter dependent upon Pr alone. This result is a consequence of the fact that f is a function of η while Ψ is a function of ξ. Solutions are

$$f = C_4 + C_3\eta^{-\frac{1}{3}} \quad \text{and} \quad \Psi = C_4 + C_1 Pr^{\frac{1}{2}} - C_2\xi^{\frac{1}{3}}. \tag{37}$$

Thus the function $f(\eta, Pr)$ varies according to $\eta^{-\frac{1}{3}}$ in the vicinity of $\eta \sim 1$. By manipulation of (4), (5), (25), (35), and (37), we obtain an expression for the upper surface Nusselt number:

$$Nu = \frac{Ra_I^{\frac{1}{4}}}{C_1 + C_4 Pr^{-\frac{1}{2}} - C_2 Pr^{-\frac{1}{3}} Ra_I^{-\frac{1}{12}}}, \tag{38}$$

where C_1, C_2, and C_4 are all Pr dependent but become independent of Pr as $Pr \to \infty$. Note that for turbulent flow, the term $C_2 Pr^{-\frac{1}{3}} Ra_I^{-\frac{1}{12}}$ is relatively small especially when Pr is very large. If, in addition, Ra_I is sufficiently large, (38) reduces to

$$Nu = K_1 Ra_I^{\frac{1}{4}}, \tag{39}$$

where K_1 is a true constant. This is the asymptotic behaviour of Nu for $Pr \gg 1$. The $\frac{1}{4}$ power-law dependence of Nu on Ra_I has been obtained by Cheung (1977) based upon a simple dimensional reasoning.

4. Low-Prandtl-number approximation

For $Pr \ll 1$, we may consider two principal flow regions: the thermal boundary-layer region $L > z > L - \delta_t$ and the turbulent core region $L - \delta_t > z > 0$. The imbedded viscous boundary layer is of trivial importance insofar as heat transfer is concerned. Since the effects of molecular or fluid properties are negligible outside the wall region, we may expect the turbulent core structure to be independent of Pr. Keeping in mind that $\delta_v < \delta_t$ the two independent variables are chosen to be $\eta = (L-z)/\delta_t$ and $\xi = \delta_t/L$.

In terms of η and ξ, the present far-field temperature profile may be constructed directly from (32). This is

$$\overline{T}_c = C_1(g\beta)^{-\frac{1}{3}}(\Phi L)^{\frac{2}{3}} L^{-\frac{1}{3}}[C_2 + (\eta\xi)^{-\frac{1}{3}}(1-\eta\xi)^{\frac{2}{3}}], \tag{40}$$

where C_1 and C_2 are parameters dependent upon Pr. Note that the thermal boundary-layer thickness δ_t, which in this case is a measure of the effective wall region, is an unknown variable to be determined. For $L > z > L-\delta_t$, we may approximate (10) by

$$|\alpha\, d\overline{T}/dz| \sim |\Phi z| \quad \text{or} \quad \alpha\Delta T_t/\delta_t \sim \Phi L, \tag{41}$$

where ΔT_t is the temperature difference across the thermal boundary layer and where the assumption of $\delta_t/L \ll 1$ has been employed to set $z \simeq L$. Based upon the above expression the following near-field temperature profile may be constructed:

$$\overline{T}_t = \alpha^{-1}\Phi L^2 \xi f(\eta, Pr) - \Delta T, \tag{42}$$

where the term ΔT comes from our convention for the zero of temperature and f is independent of Pr as $Pr \to 0$.

Let us now match the expressions for the near-field and the far-field temperatures. As before, we assume that, at high high Rayleigh number (for which $\xi \ll 1$), there is a region of overlap (i.e., $\overline{T}_t = \overline{T}_c$) where $z \sim L-\delta_t$ or $\eta \sim 1$. The existence of such an overlap region may be conceivable if here we argue that molecular conductivity and eddy conductivity are of the same order. For $\xi \ll 1$ and $\eta \sim 1$, the following relation may be obtained by manipulation of (4), (5), (40) and (42):

$$\chi(\xi f - \psi) = 2^{-\frac{1}{3}}\{C_1 C_2 + C_1(\eta\xi)^{-\frac{1}{3}}[1 + O(\xi)]\}$$

or

$$\chi(\xi f - \psi) = C_1 + C_2(\eta\xi)^{-\frac{1}{3}}[1 + O(\xi)], \tag{43}$$

where C_1 and C_2 are *new* parameters dependent upon Pr and

$$\chi = Ra_I^{\frac{1}{3}} Pr^{\frac{1}{3}} = \chi(\xi, Pr), \tag{44}$$

$$\psi = Nu^{-1} = \psi(\xi, Pr). \tag{45}$$

In writing (44) and (45), we have required $Ra_I = Ra_I(\xi, Pr)$ and $Nu = Nu(Ra_I, Pr)$. These functional forms will be examined shortly. If we differentiate (43) with respect to η and neglect the higher-order term, we get

$$\chi f_\eta = -\tfrac{1}{3}C_2(\eta\xi)^{-\frac{4}{3}} \quad \text{or} \quad -\eta^{\frac{4}{3}} f_\eta = \tfrac{1}{3}C_2 \xi^{-\frac{4}{3}}\chi^{-1} = C_3, \tag{46}$$

where f_η is the first derivative of f and C_3 is a parameter dependent upon Pr alone. Solutions are

$$\chi = (C_2/3C_3)\,\xi^{-\frac{4}{3}} \quad \text{and} \quad f = 3C_3\eta^{-\frac{1}{3}} + C_4, \tag{47}$$

where C_4 is an integration factor. Equation (43) now yields

$$\psi = \xi(C_4 - C_5\xi^{\frac{1}{3}}), \tag{48}$$

where C_5 is another parameter dependent upon Pr. Equations (44) and (47) lead to

$$\xi = A_0 Ra_I^{-\frac{1}{4}} Pr^{-\frac{1}{4}}, \tag{49}$$

where the parameter A_0 is independent of Pr as $Pr \to 0$. This is the definition of δ_t. Clearly, for $Pr \ll 1$, $\delta_t \ll L$ is a valid assumption if the condition $Ra_I \gg Pr^{-1}$ is

satisfied. We may now use (45), (48) and (49) to obtain the upper surface Nusselt number:

$$Nu = \frac{Ra_I^{\frac{1}{4}} Pr^{\frac{1}{4}}}{A_1 - A_2 Pr^{-\frac{1}{12}} Ra_I^{-\frac{1}{12}}}, \tag{50}$$

where A_1 and A_2 are Pr dependent. It can be seen from (49) and (50) that at a given Prandtl number both Nu and Ra_I can be chosen as functions of ξ alone. Thus the present analysis is self-consistent. Although (38) and (50) are quite similar in appearance, here, the term $A_2 Pr^{-\frac{1}{12}} Ra_I^{-\frac{1}{12}}$ is not negligible especially when Pr is very small. If, however, Ra_I is sufficiently high, (50) may reduce to

$$Nu = K_2 Ra_I^{\frac{1}{4}} Pr^{\frac{1}{4}}, \tag{51}$$

where K_2 is a true constant. This is the asymptotic behaviour of Nu for $Pr \ll 1$. At this extreme, the upper surface Nusselt number varies according to $Pr^{\frac{1}{4}}$ rather than the $\frac{1}{3}$ power law as in the case of Bénard flow (Kraichnan 1962; Long 1976*a*, *b*).

5. Moderate Prandtl number: comparison with experiment

For a moderate value of Pr, we may assume $\delta_t \sim \delta_v$ so that there is a single boundary-layer region at the upper surface in which molecular transport of heat and momentum dominates over the corresponding eddy transport. The behaviour of the velocity and temperature fields within the boundary layer may be determined by performing an analysis similar to the one just done. The upper surface Nusselt number may then be obtained by matching of the boundary layer and the turbulent core regions. However, we may directly generalize the expression for Nu in view of (38) and (50). This gives

$$Nu = \frac{Ra_I^{\frac{1}{4}}}{B_1 \Delta - B_2 Pr^{-\frac{1}{6}} Ra_I^{-\frac{1}{12}}}, \tag{52}$$

where Δ, B_1, and B_2 are functions of Pr and

$$\left.\begin{aligned} &\Delta \to Pr^{-\frac{1}{4}}, \quad B_i (i = 1, 2) = \text{constant} \quad \text{as} \quad Pr \to 0 \\ &\Delta \to 1 + B_3 Pr^{-\frac{1}{2}}, \quad B_i (i = 1, 2, 3) = \text{constant} \quad \text{as} \quad Pr \to \infty. \end{aligned}\right\} \tag{53}$$

For moderate Prandtl number, Δ, B_1, and B_2 may be determined from measured data. Before making a comparison with experiment, it is worthwhile at this stage to examine briefly the boundary-layer instability model of Howard (1966) based upon the present results.

For thermal convection at high Rayleigh number, Howard proposes that the molecular boundary layer is marginally stable at the wall such that a local Rayleigh number based on its thickness attains a critical value of Ra_δ, where

$$Ra_\delta = g\beta \Delta T \delta^3 / \alpha \nu. \tag{54}$$

Currently, Cheung (1978*b*) demonstrates from the existing heat transfer data that, over the explored range of Rayleigh number in the turbulent case, Ra_δ is not a constant but a function of δ/L. We shall now show that this observation is nevertheless consistent with the assumption that Ra_δ is a constant as the Rayleigh number approaches infinity. From (25) and (49), a general expression for the boundary-layer thickness may be derived. This is

$$\delta \sim \gamma Ra_I^{-\frac{1}{4}} L, \tag{55}$$

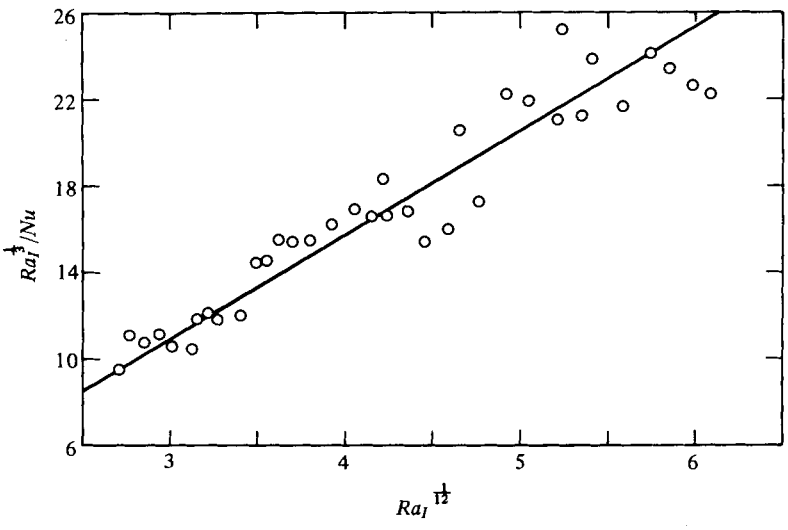

FIGURE 1. $Ra_I^{\frac{1}{3}}/Nu$ *vs.* $Ra_I^{\frac{1}{12}}$. ——, theoretical line of (60); ○, Kulacki–Nagle (1975).

where $\gamma \to Pr^{-\frac{1}{4}}$ as $Pr \to 0$ and $\gamma \to Pr^{\frac{1}{2}}$ as $Pr \to \infty$. With this expression, (54) becomes

$$Ra_\delta \sim \gamma^3 Ra_I^{\frac{1}{3}}/Nu, \tag{56}$$

where (4) and (5) have been employed. For a given Prandtl number, Ra_δ is directly proportional to $Ra_I^{\frac{1}{3}}/Nu$. From (52), we get

$$Ra_I^{\frac{1}{3}}/Nu = B_1\Delta - B_2 Pr^{-\frac{1}{3}} Ra_I^{-\frac{1}{12}}. \tag{57}$$

Thus we require $Ra_I \gg (B_2 Pr^{-\frac{1}{3}}/B_1\Delta)^{12}$ for Ra_δ to be strictly constant. At a lower Rayleigh number, Ra_δ is a function of Ra_I or, equivalently, a function of δ/L.

We may now compare the present analysis with recent experimental measurements of heat flux in water by Kulacki & Nagle (1975) and Kulacki & Emara (1977). Using two fairly entreme experiments of Kulacki & Nagle, with

$$\left.\begin{aligned} Nu &= 5{\cdot}71, \quad Ra_I = 1{\cdot}582 \times 10^5, \\ Nu &= 45{\cdot}25, \quad Ra_I = 1{\cdot}306 \times 10^9, \end{aligned}\right\} \tag{58}$$

we obtain

$$Nu = \frac{0{\cdot}207 Ra_I^{\frac{1}{3}}}{1 - 0{\cdot}751 Ra_I^{-\frac{1}{12}}}, \tag{59}$$

where $Pr \sim 6{\cdot}5$ has been assumed for water. The use of (59) can be shown to give a result which is very close to the one obtained by a least-square fit. Rewriting the above equation in the form

$$Ra_I^{\frac{1}{3}}/Nu = -3{\cdot}628 + 4{\cdot}831 Ra_I^{\frac{1}{12}}, \tag{60}$$

a straight line is obtained when plotted in the $Ra_I^{\frac{1}{3}}/Nu$–$Ra_I^{\frac{1}{12}}$ space. In figure 1, we have drawn the theoretical *line* of (60) together with the data of Kulacki & Nagle. In spite of the scatter in the experimental data, the present theory is in reasonable agreement with the observations. Note that the plot of $Ra_I^{\frac{1}{3}}/Nu$ versus $Ra_I^{\frac{1}{12}}$ tends to amplify the conventional Nu–Ra_I relationship. A small difference in the $Ra_I^{\frac{1}{3}}/Nu$–$Ra_I^{\frac{1}{12}}$

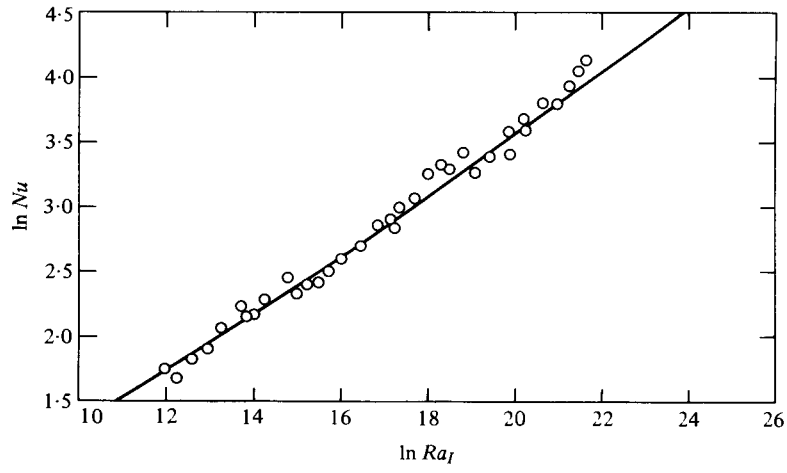

FIGURE 2. ln Nu *vs.* ln Ra_I. ——, theoretical curve of (59); ○, Kulacki–Nagle (1975).

expression would, therefore, lead to a negligible error in the calculated Nusselt number. As shown in figure 2, the data of Kulacki & Nagle appear to be fairly well correlated by the theoretical *curve* when presented in the Nu–Ra_1 space.

A slightly different expression for Nu may be obtained using the data of Kulacki & Emara. We get

$$Nu = \frac{0{\cdot}206 Ra_I^{\frac{1}{4}}}{1 - 0{\cdot}847 Ra_I^{-\frac{1}{12}}}, \tag{61}$$

where we have employed the following two sets of experiments:

$$\left.\begin{aligned} Nu &= 5{\cdot}30, \quad Ra_I = 1{\cdot}065 \times 10^5, \\ Nu &= 143{\cdot}27, \quad Ra_I = 1{\cdot}546 \times 10^{11}. \end{aligned}\right\} \tag{62}$$

Again, the use of (61) can be shown to give a result which is very close to the one obtained by a least-square fit. Rewriting the equation in the form

$$Ra_I^{\frac{1}{4}}/Nu = -4{\cdot}112 + 4{\cdot}854 Ra_I^{\frac{1}{12}}, \tag{63}$$

a straight line is obtained when plotted in the $Ra_I^{\frac{1}{4}}/Nu$–$Ra_I^{\frac{1}{12}}$ space. Note that a value of Ra_I as high as $2{\cdot}17 \times 10^{12}$ has been achieved in the work of Kulacki & Emara, but for $Ra_I > 1{\cdot}546 \times 10^{11}$, the effect of property variation has been found to be quite large. Therefore, we do not intend to analyse that portion of the data. In figure 3, we have drawn the theoretical *line* of (63) together with the data of Kulacki & Emara. Although the data appear to be somewhat scattered, the range of the internal Rayleigh number covered in this case is sufficiently wide to lend real support to the $Ra_I^{-\frac{1}{12}}$ term in (52). Again, the agreement between the present theory and the experimental data becomes highly satisfactory when compared in the conventional Nu–Ra_I space, as can be seen in figure 4. Moreover, within the explored range of Ra_I, the theoretical *curve* itself may well be approximated by the $Ra_I^{0.227}$ law (Kulacki & Emara 1977). This explains the fact that often the measured data can be correlated successfully by a simple power-law relationship, which has no theoretical basis. To further illustrate this point, we have reconstructed the theoretical curve of (61) in the $Ra_I^{\frac{1}{4}}/Nu$–Ra_I

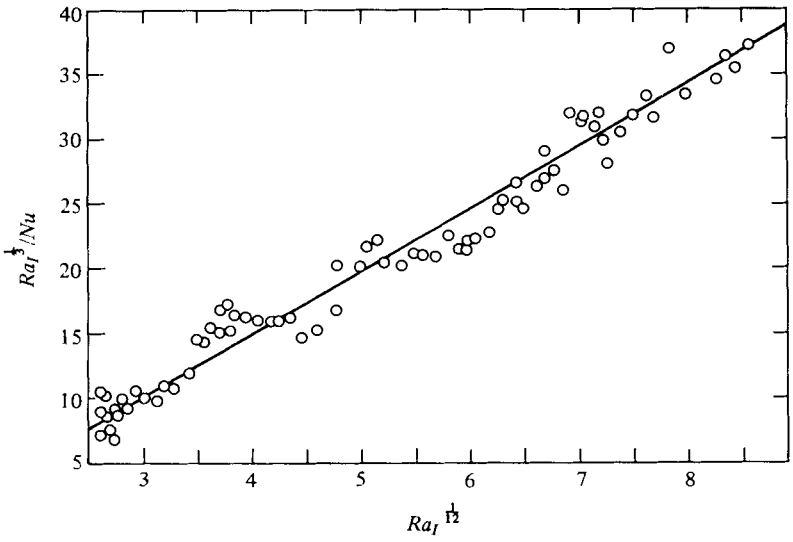

FIGURE 3. $Ra_I^{\frac{1}{3}}/Nu$ *vs.* $Ra_I^{\frac{1}{12}}$. ——, theoretical line of (63); ○, Kulacki–Emara (1977).

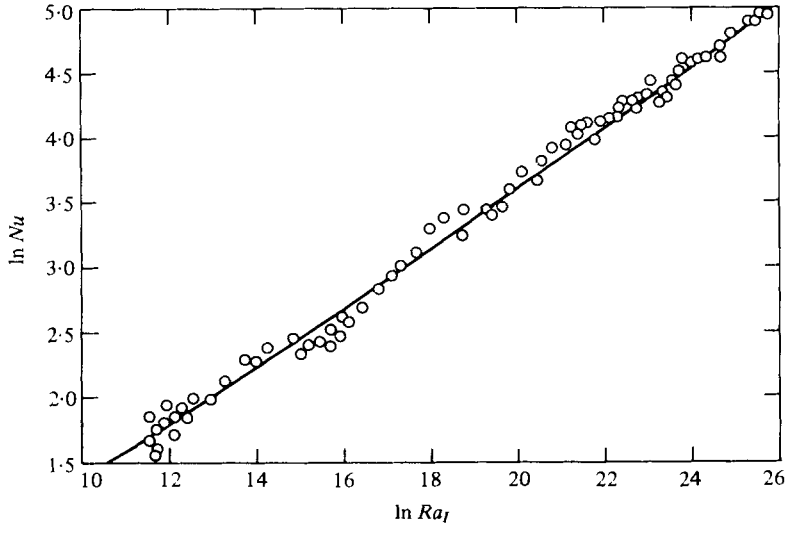

FIGURE 4. ln Nu *vs.* ln Ra_I. ——, theoretical curve of (61); ○, Kulacki–Emara (1977).

space over a rather wide scale of Ra_I, ranging from 10^5 to 10^{39}, as shown in figure 5. This plot shows exactly how the Nu–Ra_I relation deviates from the asymptotic behaviour at a not-sufficiently high Rayleigh number. Clearly, we may approximate the theoretical curve by a number of successive straight-line segments. In particular, we may have

$$\left.\begin{aligned} Nu &\sim Ra_I^{0.227} \quad \text{for} \quad 10^5 < Ra_I < 10^{11}, \\ Nu &\sim Ra_I^{0.245} \quad \text{for} \quad 10^{12} < Ra_I < 10^{22}, \\ Nu &\sim Ra_I^{0.250} \quad \text{for} \quad Ra_I \geqslant 10^{23}. \end{aligned}\right\} \tag{64}$$

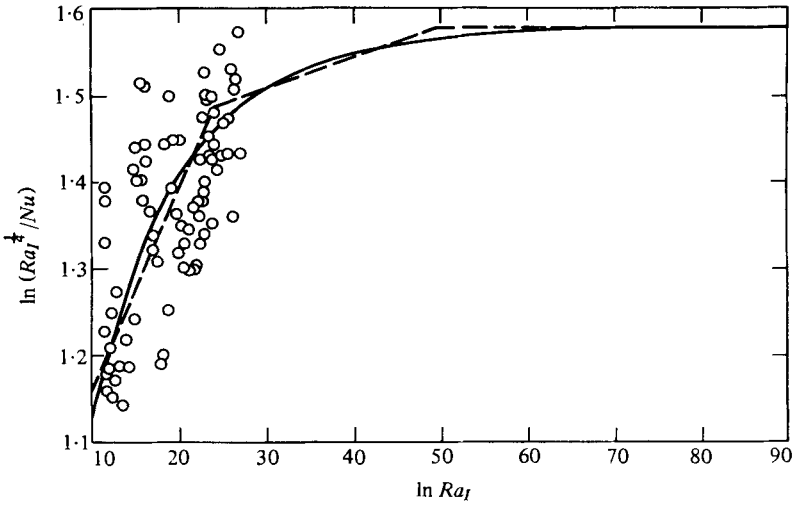

FIGURE 5. ln $(Ra_I^{\frac{1}{4}}/Nu)$ *vs.* ln Ra_I. ——, theoretical curve of (61); – – –, power-law expression (64); ○, Kulacki–Emara (1977).

These segments, when presented in the conventional Nu–Ra_I space, become identical to (61). Note that the plot of $Ra_I^{\frac{1}{4}}/Nu$ versus Ra_I greatly amplifies the differences among various experimental measurements and thus results in a considerable scatter of the data. As a result, the asymptotic value of $Ra_I^{\frac{1}{4}}/Nu$, which in this case is equal to 4·854, cannot be determined by the heat-transfer data alone. This indicates that a simple dimensional analysis may only be used to predict the $Ra_I^{\frac{1}{4}}$ behaviour in a *qualitative* manner.

We have remarked that there are sensible departures from the asymptotic behaviour at the Rayleigh numbers so far explored. We may now estimate the magnitude of Ra_I for (59) and (61) to yield a close approximation to the $Ra_I^{\frac{1}{4}}$ law. From (59), we get $Ra_I > 3{\cdot}2 \times 10^{22}$ for an error of less than 1 % in the upper surface Nusselt number. The corresponding inequality based upon (61) is $Ra_I > 1{\cdot}4 \times 10^{23}$. In view of (56), these also are the conditions for Ra_δ to be strictly constant. Far below these limits, the assumption of a constant Ra_δ is a very crude approximation (Sparrow, Husar & Goldstein 1970; Davenport & King 1975; Manton 1975).

6. Discussion and summary

A simple theory has been developed for the dependence of the upper surface Nusselt number upon Prandtl number and internal Rayleigh number in turbulent thermal convection in a horizontal fluid layer heated from within. The behaviour of the velocity and temperature fields in various flow regions within the layer has been determined for both high and low Prandtl numbers. The results indicate that the present turbulence structure, particularly the variation of mean turbulent temperature, r.m.s. vertical velocity, and the production of turbulent energy in the core region, is quite different from that of Rayleigh–Bénard convection, although buoyancy is the main driving force in both cases. On the other hand, the boundary-layer-dominant aspect and the convective pattern within and adjacent to the wall region are quite the

	Rayleigh–Bénard convection	Heat source-driven convection
Total heat flux	Constant	Φz
Production of turbulent energy in the core	Constant	Φz
R.m.s. vertical velocity (turbulent core region)	$(L-z)^{\frac{1}{3}}$	$[z(L-z)]^{\frac{1}{3}}$
Turbulent core temperature	$(L-z)^{-\frac{1}{3}}$	$z^{\frac{2}{3}}(L-z)^{-\frac{1}{3}}$
Asymptotic law of dependence of heat transport (large Pr)	$Ra^{\frac{1}{3}}$	$Ra_I^{\frac{1}{4}}$
Asymptotic law of dependence of heat transport (low Pr)	$Ra^{\frac{1}{2}}Pr^{\frac{1}{2}}$	$Ra_I^{\frac{1}{5}}Pr^{\frac{1}{2}}$

$Pr = \nu/\alpha$, $Ra = g\beta\Delta TL^3/\alpha\nu$, $Ra_I = g\beta\Phi L^5/2\alpha^2\nu$.

TABLE 1. Comparison between heat source-driven and Rayleigh–Bénard convection.

same for the two buoyancy-induced motions. This may be an explanation to the observations that the processes of upward heat transfer in bottom-heated and internally heated fluid layers are qualitatively similar yet quantitatively different (Cheung 1978*b*; Bergholz *et al.* 1979). A brief comparison between heat source-driven and Rayleigh–Bénard convection is summarized in table 1. In addition, we have examined the validity of the boundary-layer instability model of Howard (1966) based upon the present theory. For Ra_δ to be strictly constant, Ra_I has to be sufficiently high (which is of the order 10^{23} for water). At a lower Rayleigh number, Ra_δ is a function of δ/L and this results in departures from the asymptotic $Ra_I^{\frac{1}{4}}$ law. A closed-form expression for the deviated Nu–Ra_I relation has been obtained and discussed along with experiment. Finally, we have shown that the empirical power-law relation so far employed in experimental correlation is an adequate expression for Nu within a finite range of Ra_I.

Owing to the lack of experimental data on the detailed structure of turbulence, many elements of the present analysis have been inferred from the corresponding case of Bénard flow. The order-of-magnitude analysis employed in the boundary-layer region, for example, has been used by Long (1976*a*, *b*) for the case of Rayleigh-Bénard flow. Similarly, the mixing-length treatment employed in the turbulent core region has been used by Priestley (1959) and Kraichnan (1962). Moreover, the same three cases of large, small, and intermediate Prandtl numbers considered in this study have been treated in Kraichnan's paper (1962) on Bénard convection at large Rayleigh numbers. The present approach, however, differs markedly from that of Kraichnan in that here no assumption is made regarding the transition Péclet and Reynolds numbers. The rate of heat transfer in the present case is determined completely by matching of the boundary layer and the turbulent core flows. In so doing, we are not only able to obtain the asymptotic law of heat transport at a sufficiently high Rayleigh number but are also able to understand how and why the Nu–Ra_I relation deviates from the asymptotic behaviour at lower Rayleigh numbers. The latter information could not be obtained using Kraichnan's approach. It should be noted that although there is good agreement between the present theory and the experimental results (Kulacki & Nagle 1975; Kulacki & Emara 1977), there is lack of rigorous theoretical basis for the existence of an overlap region in which we match the expressions for the near-field and far-field temperatures. Further work is needed in this area.

The author wishes to thank Ms Marilyn Goldman and Mrs Gloria Ridges for typing and manuscript preparation. This research was performed under the auspices of the U.S. Department of Energy.

The submitted manuscript has been authored by a contractor of the U.S. Government under contract no. W-31-109-ENG-38. Accordingly, the U.S. Government retains a non-exclusive, royalty-free license to publish or reproduce the published form of this contribution, or allow others to do so, for U.S. Government purposes.

REFERENCES

BERGHOLZ, R. F., CHEN, M. M. & CHEUNG, F. B. 1979 Generalization of heat transfer results for turbulent free convection adjacent to horizontal surfaces. *Int. J. Heat Mass Transfer* **22**, 763–769.

CHEUNG, F. B. 1977 Natural convection in a volumetrically heated fluid layer at high Rayleigh numbers. *Int. J. Heat Mass Transfer* **20**, 499–506.

CHEUNG, F. B. 1978*a* Turbulent natural convection in a horizontal fluid layer with time dependent volumetric energy sources *A.I.A.A./A.S.M.E. Thermophysics & Heat Transfer Conf., Palo Alto*, paper No. 78–HT-6.

CHEUNG, F. B. 1978*b* Correlation equations for turbulent thermal convection in a horizontal fluid layer heated internally and from below. *J. Heat Transfer* **100**, 416–422.

CHU, T. Y. & GOLDSTEIN, R. J. 1973 Turbulent convection in a horizontal layer of water. *J. Fluid Mech.* **60**, 141–159.

DAVENPORT, F. & KING, C. J. 1975 A note on Hoard's model for turbulent natural convection. *J. Heat Transfer* **97**, 476–478.

FIEDLER, H. & WILLE, R. 1971 Wärmetransport bie frier Konvektion in einer horizontalen Flussigkeitsschicht mit Volumenheizung, Teil 1: Integraler Wärmetransport. *Rep. Dtsch Forschungs Varsuchsanstalt Luft-Raumfahrt, Inst. Turbulenzfenschung, Berlin.*

GARON, A. M. & GOLDSTEIN, R. J. 1973 Velocity and heat transfer measurements in thermal convection. *Phys. Fluids* **16**, 1818–1825.

HERRING, J. R. 1964 Investigation of problems in thermal convection: Rigid boundaries. *J. Atmos. Sci.* **21**, 277–290.

HOWARD, L. N. 1966 Convection at high Rayleigh number. In *Proc. 11th Cong. Appl. Mech.* (ed. H. Görtler), pp. 1109–1115.

KRAICHNAN, R. H. 1962 Turbulent thermal convection at arbitrary Prandtl number. *Phys. Fluids* **5**, 1374–1389.

KULACKI, F. A. & EMARA, A. A. 1977 Steady and transient thermal convection in a fluid layer with uniform volumetric energy sources. *J. Fluid Mech.* **83**, 375–395.

KULACKI, F. A. & NAGLE, M. E. 1975 Natural convection in a horizontal fluid layer with volumetric energy sources. *J. Heat Transfer* **91**, 204–211.

LONG, R. R. 1976*a* The relation between Nusselt number and Rayleigh number in turbulent thermal convection. *J. Fluid Mech.* **73**, 445–451.

LONG, R. R. 1976*b* Theories of turbulent thermal convection. *Heat Transfer and Turbulent Buoyant Convection* (ed. D. B. Spalding & N. Afgan), pp. 79–91. Hemisphere.

MALKUS, W. V. R. 1954 The heat transport and spectrum of thermal turbulence. *Proc. Roy. Soc.* A **225**, 196–212.

MANTON, M. J. 1975 On the high Rayleigh number heating of a fluid above a horizontal surface. *Appl. Sci. Res.* **31**, 267–277.

PRIESTLEY, C. H. B. 1959 *Turbulent Transfer in the Lower Atmosphere.* University of Chicago Press.

SPARROW, E. M., HUSAR, R. B. & GOLDSTEIN, R. J. 1970 Observations and other characteristics of thermals. *J. Fluid Mech.* **41**, 793–800.

SPIEGEL, E. A. 1971 Convection in stars, I. Basic Boussinesq convection. *Ann. Rev. Astronomy & Astrophys.* **9**, 323–352.

TENNEKES, H. & LUMLEY, J. L. 1972 *A First Course in Turbulence.* Massachusetts Institute of Technology Press.

THRELFALL, D. C. 1975 Free convection in low-temperature gaseous helium. *J. Fluid Mech.* **67**, 17–28.